Taylor & Francis
Taylor & Francis Group

Automatika

Journal for Control, Measurement, Electronics, Computing and Communications

ISSN: 0005-1144 (Print) 1848-3380 (Online) Journal homepage: https://www.tandfonline.com/loi/taut20

Constrained field-oriented control of permanent magnet synchronous machine with field-weakening utilizing a reference governor

Tino Jerčić, Šandor Ileš, Damir Žarko & Jadranko Matuško

To cite this article: Tino Jerčić, Šandor Ileš, Damir Žarko & Jadranko Matuško (2017) Constrained field-oriented control of permanent magnet synchronous machine with field-weakening utilizing a reference governor, Automatika, 58:4, 439-449, DOI: 10.1080/00051144.2018.1453441

To link to this article: https://doi.org/10.1080/00051144.2018.1453441

© 2018 The Author(s). Published by Informa UK Limited, trading as Taylor & Francis Group

Published online: 31 May 2018.

Submit your article to this journal

Article views: 919

View related articles

View Crossmark data

Full Terms & Conditions of access and use can be found at
https://www.tandfonline.com/action/journalInformation?journalCode=taut20

AUTOMATIKA, 2017
VOL. 58, NO. 4, 439–449
https://doi.org/10.1080/00051144.2018.1453441

REGULAR PAPER

OPEN ACCESS Check for updates

Constrained field-oriented control of permanent magnet synchronous machine with field-weakening utilizing a reference governor

Tino Jerčić, Šandor Ileš, Damir Žarko and Jadranko Matuško

Faculty of Electrical Engineering and Computing, Department of Electrical Machines Drives and Automation, University of Zagreb, Zagreb, Croatia

ABSTRACT

This paper presents a complete solution for constrained control of a permanent magnet synchronous machine. It utilizes field-oriented control with proportional-integral current controllers tuned to obtain a fast transient response and zero steady-state error. To ensure constraint satisfaction in the steady state, a novel field-weakening algorithm which is robust to flux linkage uncertainty is introduced. Field weakening problem is formulated as an optimization problem which is solved online using projected fast gradient method. To ensure constraint satisfaction during current transients, an additional device called current reference governor is added to the existing control loops. The constraint satisfaction is achieved by altering the reference signal. The reference governor is formulated as a simple optimization problem whose objective is to minimize the difference between the true reference and a modified one. The proposed method is implemented on Texas instruments F28343 200 MHz microcontroller and experimentally verified on a surface mounted permanent magnet synchronous machine.

ARTICLE HISTORY
Received 31 October 2017
Accepted 1 March 2018

KEYWORDS
Permanent magnet machines; vector control; optimization; PI control; nonlinear control systems; field weakening

1. Introduction

Permanent magnet synchronous machine (PMSM), due to its inherently high torque density and premium efficiency stands out as a motor of choice in a wide array of applications and especially proves as a perfect fit in electric traction applications. In order to fully utilize its advantages a proper control system must be employed.

In traction applications, the main objective is to ensure reaching the reference torque with a good dynamic performance while achieving loss minimization in the steady state. This can be achieved by a proper current control algorithm which must respect PMSM drive voltage and current limits.

With addition of loss minimization requirement, the control strategy of a PMSM can be divided into three segments: an algorithm for finding the optimal current vector which minimizes the copper losses or total copper and iron losses in a steady state, field-weakening algorithm which ensures that voltage constraints are not violated in steady state, and a control algorithm responsible for tracking of reference current trajectory.

An algorithm for finding the optimum current vector is often given in a form of pre-calculated look-up table [1], analytical solution [2] or some sort of on-line loss minimization search algorithm [3,4].

Control techniques for tracking the current trajectory based on vector/field-oriented control (FOC) or direct torque control (DTC) are most commonly used for PMSMs [5,6].

In FOC, the control system usually employs proportional-integral (PI) controllers with decoupling terms and pulse-width modulation to keep the currents at their desired values. The main advantage of FOC is in its modularity, flexibility, robustness regarding parameter variation and low computational burden, which makes it an industry standard in control of PMSMs. However, voltage and current constraints are not considered in the design stage. Instead, usually antiwindup techniques, dynamic over-modulation and even decreasing of the controller gain are used [7,8]. Over-modulation inevitably leads to increase in losses during transient operation, while any decrease of controller gain is followed by a performance deterioration. Various antiwindup techniques such as realizable references (back-calculation) are commonly used to alleviate the problem of saturation [7,9]. However, by using such techniques the control designer cannot influence in which way the allowable reference is reached. Furthermore, such techniques cannot handle current constraints.

On the other hand, the DTC uses flux and torque hysteresis controllers and a look-up table to directly control the transistor switching. The current constraints are handled using the hysteresis band while the voltage constraints are not considered.

Recently, advanced control techniques have also been developed for controlling this type of electric machines in order to handle constraints. Among them

CONTACT Tino Jerčić tino.jercic@fer.hr Faculty of Electrical Engineering and Computing, Department of Electrical Machines Drives and Automation, University of Zagreb, Zagreb, Croatia

© 2018 The Author(s). Published by Informa UK Limited, trading as Taylor & Francis Group
This is an Open Access article distributed under the terms of the Creative Commons Attribution License (http://creativecommons.org/licenses/by/4.0/), which permits unrestricted use, distribution, and reproduction in any medium, provided the original work is properly cited.

the most notable is model predictive control (MPC). In general, MPC approaches for PMSM can be divided into two groups: namely the finite control-set (FCS-MPC) and continuous control-set (CCS-MPC) methods [10,11]. FCS-MPC takes into account the discrete nature of the power converter. By checking all the possible combinations of switches, taking into account the cost function and constraints, the optimal switching of the power converter can be found [12]. However, this is limited to short prediction horizons due to the combinatorial nature of the problem. The main disadvantage of such control scheme is variable switching frequency of the converter and ringing. On the other hand, similar to FOC, CCS-MPC abstracts away the discrete nature of the power converter by using pulse-width modulation. The CCS-MPC can be implemented as an explicit MPC which requires a high amount of memory, or as on-line MPC which, on the other hand, requires a fast online solver [13–15].

An alternative and computationally less demanding approach to cope with constraints is to keep the existing control loop and employ a so-called reference governor. Its task is to alter the external reference input to the existing control loops in order to satisfy the constraints [16,17]. The altered reference input is obtained by solving a simple optimization problem at every sampling instant where the objective function is specified by the control designer. The most commonly used objective function is to minimally alter the reference input to satisfy the constraints. In the absence of constraints the performance remains the same as with the original controller. The reference governor and its utilization in PMSMs is investigated in simulation in our conference paper [18]. The voltage constraint is linearized which results in underutilization of motor voltage and therefore in somewhat conservative control law. Furthermore, the field-weakening operation is not investigated in the aforementioned paper.

To ensure feasibility of reference current vector, in context of voltage constraint satisfaction in a steady state, field-weakening algorithm is required. The methods of current control in the field-weakening (FW) area, which are based on FOC control, can be classified into feed-forward (FF) methods, feedback methods (FB) and FF/FB hybrid methods.

The FF method calculates the feasible current vector based on the machine model, desired torque, DC link voltage and measured speed [19–21]. This method requires accurate knowledge of machine model and its parameters, resulting in faulty FW operation in the case of errors in the presumed machine model and/or parameters.

Feedback methods [22–24] use outputs from the current controller (reference voltages in d and q axes) as a feedback information to calculate the reference current vector required for field-weakening operation. This method does not require accurate knowledge of machine parameters. The drawback of the feedback method is a slow field-weakening dynamics which creates problems during transitional states due to possible premature activation of field-weakening operation during current transients, when rapid change of current reference (i.e. desired torque reference) results in the voltage constraint violation and saturation of current controllers. The field-weakening operation of feedback methods is activated when the limits are already violated.

In the hybrid methods according to [25,26], the feed-forward component is utilized in the form of 2D look-up tables and used to determine the current vector according to the available flux which is calculated from the DC link voltage and rotor speed. With the use of feed-forward component, good dynamic response of field-weakening operation is achieved, while the feedback is added to compensate the influence of mathematical model or machine parameter uncertainty. The flaws of this method are related to problems considering acquiring the feed-forward 2D look-up tables and memory required to save them, along with computing requirements in real-time implementation.

This paper builds on the results presented in [18] and provides a complete solution for constrained field-oriented torque control. Similar to [18], a reference governor is employed to ensure constraint satisfaction during transients. Unlike [18], the voltage constraint is not linearized which results in a less conservative control law and a faster transient response. In addition, to ensure constraint satisfaction in a steady state a novel hybrid field-weakening algorithm, robust to machine parameter uncertainty and error caused by saturation effects, temperature effect on permanent magnet flux linkage and/or simply erroneous parameter identification, is introduced. Field weakening problem is formulated as an optimization problem, the solution of which is found using projected fast gradient method. The proposed method is implemented on Texas instruments F28343 200 MHz microcontroller and experimentally verified on surface mounted permanent magnet synchronous machine.

The paper is organized as follows: In Section 2 the standard FOC of PMSM is presented, Section 3 presents a reference governor as a solution for constraint satisfaction during transients, Section 4 presents a novel field-weakening solution which ensures constraint satisfaction in the steady state, Section 5 presents simulation and experimental results and Section 6 concludes the paper.

2. FOC of a PMSM

2.1. Mathematical model

Mathematical model of a synchronous permanent magnet motor can be described in the $d-q$ coordinate

system which rotates in synchronism with the electrical angular speed of the rotor (Figure 1). Motor equations, neglecting the core losses, are given by

$$v_d = R_s i_d + \frac{\mathrm{d}}{\mathrm{d}t}\Psi_d - \omega_e \Psi_q, \tag{1}$$

$$v_q = R_s i_q + \frac{\mathrm{d}}{\mathrm{d}t}\Psi_q + \omega_e \Psi_d, \tag{2}$$

$$T_e = \frac{3}{2} p[\Psi_d i_q - \Psi_q i_d], \tag{3}$$

where i_d and i_q are the d and q axis currents, ω_e is the electrical angular velocity, p is the number of pole pairs, v_d and v_q are the d and q axis voltages, and T_e is the electromagnetic torque. Ψ_d and Ψ_q are the direct and quadrature axis flux linkages which are function of both, d and q axis current components

$$\Psi_d = f_d(i_d, i_q), \tag{4}$$

$$\Psi_q = f_q(i_d, i_q). \tag{5}$$

For the control synthesis purpose, the q axis component of permanent magnet flux and cross-inductances are neglected (i.e. $\Psi_{mq} = 0$ and $L_{dq} = L_{qd} = 0$). Saturation effects are also neglected presuming the constant value of inductances L_d and L_q and constant value of permanent magnet flux component in the d axis Ψ_{md}, i.e. through linearization

$$\Psi_d \approx \Psi_{md} + L_d i_d, \tag{6}$$

$$\Psi_q \approx L_q i_q, \tag{7}$$

resulting in PMSM model suitable for control algorithm development

$$v_d = R_s i_d + L_d \frac{\mathrm{d}}{\mathrm{d}t} i_d - \omega_e L_q i_q, \tag{8}$$

$$v_q = R_s i_q + L_q \frac{\mathrm{d}}{\mathrm{d}t} i_q + \omega_e L_d i_d + \omega_e \Psi_{md}, \tag{9}$$

$$T_e = \frac{3}{2} p \left[\Psi_{md} + (L_d - L_q) i_d\right] i_q. \tag{10}$$

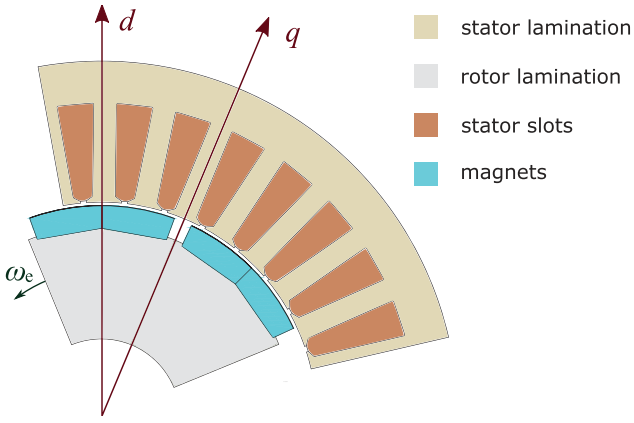

Figure 1. The *d*-*q* coordinate system shown on an SPMSM rotor.

2.2. Control structure

In the remainder of this section the proposed control method is described.

There is a direct correlation between current vector in the dq coordinate system and the produced electromagnetic torque, therefore the torque control problem of PMSM translates to a current control in the dq system. In the classical current vector control structure (Figure 2), the currents are regulated by two separate d and q current control loops with PI controllers. Due to coupling between d and q axis, these two loops are not independent. In order to allow separate control of currents in the d and q axis, the decoupling is performed (Figure 3).

The decoupling allows the use of linear control theory for the synthesis of the controller. The augmented PI controllers with decoupling can be written as

$$\frac{\mathrm{d}}{\mathrm{d}t} I_{ed} = (i_d^* - i_d), \tag{11}$$

$$\frac{\mathrm{d}}{\mathrm{d}t} I_{eq} = (i_q^* - i_q), \tag{12}$$

$$v_d^*(t) = K_{pd}(i_d^* - i_d) + K_{id} I_{ed} - \omega_e L_q i_q, \tag{13}$$

$$v_q^*(t) = K_{pq}(i_q^* - i_q) + K_{iq} I_{eq} + \omega_e L_d i_d + \omega_e \Psi_{md}, \tag{14}$$

where K_{pd}, K_{pq}, K_{id}, K_{iq} are the proportional and integral gains of the d and q axis current PI controllers respectively, while I_{ed} and I_{eq} are the accumulated d and q axis current errors.

Using the aforementioned control law, the cancellation of nonlinear terms in the system equations (8)

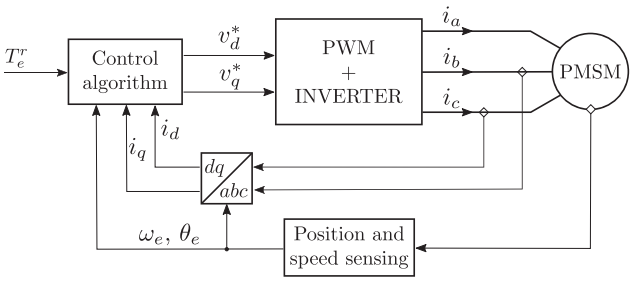

Figure 2. Field-oriented control of PMSM

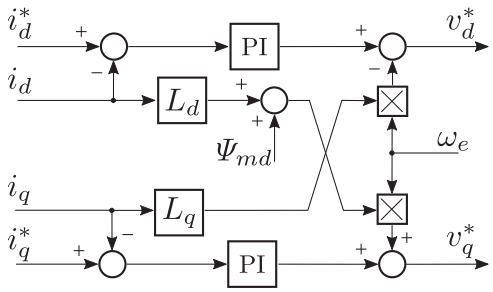

Figure 3. The *d* and *q* axis current PI controller with decoupling.

and (9) occurs, and the closed loop system can be written in the form

$$L_d\frac{\mathrm{d}}{\mathrm{d}t}i_d + R_s i_d = K_{pd}(i_d^* - i_d) + K_{id}I_{ed}, \tag{15}$$

$$L_q\frac{\mathrm{d}}{\mathrm{d}t}i_q + R_s i_q = K_{pq}(i_q^* - i_q) + K_{iq}I_{eq}. \tag{16}$$

Conventionally, the PI controllers are tuned to achieve fast and well damped transient response without considering constraints, which are namely, in the context of PMSM control, current and voltage constraints

$$i_d^2 + i_q^2 \le I_{\max}^2, \tag{17}$$

$$v_d^2 + v_q^2 \le V_{\max}^2, \tag{18}$$

where $I_{\max}$ is the maximum current amplitude while $V_{\max}$ is the maximum voltage available from the inverter (for space vector modulation and star connection $V_{\max} = V_{\mathrm{DC}}/\sqrt{3}$, where V_{DC} is the DC link voltage). Machine can usually, for limited amount of time, withstand the current several times larger then its rated value. Machine ability to operate with currents larger than rated value depends on machine's thermal conditions and thermal capacitance, making the maximum permissible current hard to define. In the literature, the current limit is often neglected or treated in a form of soft constraint.

To analyse the transient response of the closed-loop system and satisfaction of the constraints, the system dynamics can be rewritten in a state-space form. This analysis is performed during operation of the machine on a microcontroller and therefore rewritten as a discrete-time autonomous dynamical system in a state-space form. Using the Euler-forward discretization, with sampling time T_s, the model (15)–(16) can be represented as follows

$$x(k+1) = Ax(k), \tag{19}$$

where $x = [i_d\, i_q\, I_{ed}\, I_{eq}\, i_d^*\, i_q^*]^{\mathrm{T}}$ and the matrix A is given as

$$A = \begin{bmatrix} -\frac{T_s}{L_d}(R_s + K_{pd}) + 1 & 0 & \frac{T_s K_{id}}{L_d} & 0 & \frac{T_s K_{pd}}{L_d} & 0 \\ 0 & -\frac{T_s}{L_q}(R_s + K_{pq}) + 1 & 0 & \frac{T_s K_{iq}}{L_q} & 0 & \frac{T_s K_{pq}}{L_q} \\ -T_s & 0 & 1 & 0 & T_s & 0 \\ 0 & -T_s & 0 & 1 & 0 & T_s \\ 0 & 0 & 0 & 0 & 1 & 0 \\ 0 & 0 & 0 & 0 & 0 & 1 \end{bmatrix}. \tag{20}$$

Based on the derived model, the idea is to compute the references which ensure tracking of the desired torque while at the same time minimizing losses and ensuring satisfaction of constraints.

To ensure reachability of torque and corresponding loss minimizing current vector references, a field-weakening algorithm is introduced in the classical control system of PMSM. The task of the proposed field-weakening algorithm is to guarantee satisfaction of the current and voltage constraints in a steady state. Even though the proposed field-weakening algorithm ensures constraint satisfaction in a steady state, the PI controller with decoupling still presents a potential problem for constraint satisfaction during current transients. Therefore, to ensure that control system respects voltage limits even during current transients, a device called reference governor is added into an existing PMSM control structure. In order to simplify the reference governor algorithm, its implementation and to ease its computational burden, the current constraints are treated as a soft constraint handled by field-weakening algorithm. The complete control structure is shown in Figure 4 and all the components are described in the sequel.

3. Reference governor

A reference governor approach considers an asymptotically stable closed-loop discrete-time system

$$\begin{aligned} x(k+1) &= f(x(k), r(k)), \\ y(k) &= g(x(k), r(k)), \end{aligned} \tag{21}$$

where $x(k)$ represents the state, $y(k)$ represents the output, and $r(k)$ represents the corresponding reference signal, subject to constraints $y(k+j) \in \mathcal{Y}, j \in \mathbb{Z}_+$, where $\mathcal{Y}$ is a set representing the constraints. In order to ensure the constraint satisfaction, the desired reference signal has to be suitably modified. In other words, the reference governor generates a new reference signal $v(k)$ following the two key principles: if $v(k)$ is kept constant, constraints are not violated and $v(k)$ is a close approximation of the original reference signal $r(k)$. The aforementioned principles can be mathematically described as follows

$$\begin{aligned} &\min J(v(k), r(k)) \\ &\text{subject to } x(k+1) \in \mathcal{O}_\infty, \end{aligned} \tag{22}$$

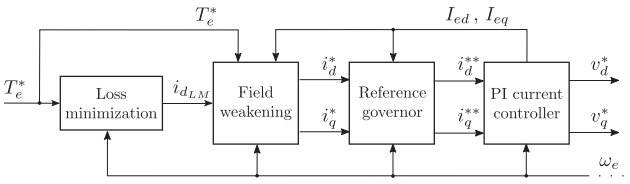

Figure 4. Field weakening and current reference governor position in control scheme.

where J is the cost function which ensures that the modified reference signal is as close as possible to the desired reference signal. In order to ensure constraint satisfaction at all times, usually the maximum output admissible set $\mathcal{O}_\infty$ [17] is used. The maximum output admissible set is a set of all states $x(k)$ and constant reference signals $\bar{v}$ for which system constraints are not violated

$$\mathcal{O}_\infty = \{(\bar{v}, x(k)) : y(k+j) \in \mathcal{Y}, (\bar{v}, x(k+j)) \in \mathcal{O}_\infty, \\ v(k+j) = \bar{v}, j \in \mathbb{Z}_+\}. \tag{23}$$

The reference governor control scheme is shown in Figure 5.

3.1. Reference governor for constrained current control of PMSM

The following objective function is proposed for the purpose of applying the reference governor to a PMSM

$$J(v(k), r(k)) = (r(k) - v(k))^T (r(k) - v(k)). \tag{24}$$

In order to guarantee the recursive feasibility the maximum output admissible set has to be found. Using the controller dynamics (11)–(14), the corresponding voltage constraint (18) can be rewritten as the nonlinear state constraint

$$\mathcal{X} = \{x : f_V(x, \omega_e) \leq V_{\max}^2\}, \tag{25}$$

where $f_V(x, \omega_e)$ is defined as

$$f_V(x, \omega_e) = v_d^2(x, \omega_e) + v_q^2(x, \omega_e) = (A_d x)^2 \\ + (A_q x + \omega_e \Psi_{md})^2, \tag{26}$$

while matrices A_d and A_q are given as

$$\begin{aligned} A_d &= [-K_{pd} \quad -\omega_e L_q \quad K_{id} \quad 0 \quad K_{pd} \quad 0], \\ A_q &= [\omega_e L_d \quad -K_{pq} \quad 0 \quad K_{iq} \quad 0 \quad K_{pq}]. \end{aligned} \tag{27}$$

The maximum output admissible set can be calculated using the following recursion

$$\mathcal{S}_{k+1} = \{x : x \in \mathcal{S}_k, Ax \in S_k\}, \quad k = 1, \ldots, k_{\max}, \tag{28}$$

where

$$\mathcal{S}_0 = \mathcal{X}, \tag{29}$$

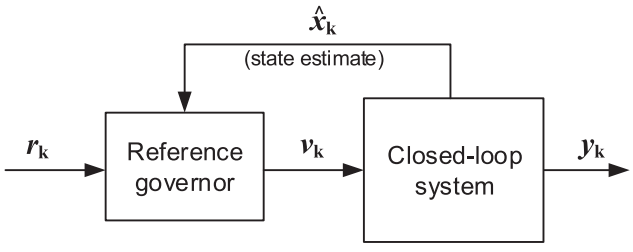

Figure 5. Reference governor applied to a closed loop system.

and $k_{\max}$ is a number for which $\mathcal{S}_{k_{\max}} = \mathcal{S}_{k_{\max}-1}$. The maximum output admissible set is then obtained as

$$O_\infty = S_{k_{\max}}. \tag{30}$$

Since the closed loop system is described as an autonomous system (19), the maximum output admissible set is defined by the following set of constraints

$$\begin{aligned} f_V(x, \omega_e) &\leq V_{\max}^2, \\ f_V(Ax, \omega_e) &\leq V_{\max}^2, \\ f_V(A^2 x, \omega_e) &\leq V_{\max}^2, \\ &\ldots \\ f_V(A^{k_{\max}} x, \omega_e) &\leq V_{\max}^2. \end{aligned} \tag{31}$$

Taking all the aforementioned into account the corresponding maximum output admissible set can be calculated offline for a single operating point defined by the motor speed, and updated online if the operating point changes.

At every time instant, the set of admissible reference signals is obtained as an intersection of the maximum output admissible set with the measured values $[i_d \; i_q \; I_{ed} \; I_{eq}]^{\mathrm{T}}$, the projection of the desired reference signal r_k onto the resulting set is performed and applied to the closed loop system.

4. Field weakening operation of PMSM

Combining the voltage constraint defined by (18) and machine model according to (8) and (9), voltage constraint in a steady state can be mapped onto current vector constraint

$$(R_s i_d - \omega_e \Psi_q)^2 + (R_s i_q + \omega_e \Psi_d)^2 \leq V_m^2. \tag{32}$$

Neglecting the voltage drop across winding resistance R_s, along with linearization of the flux linkage according to (6) and (7), the voltage constraint equation (32) takes the form of the ellipse formally known as voltage ellipse with its centre at $(\Psi_{md}/L_d, 0)$

$$(L_q i_q)^2 + (L_d i_d + \Psi_{md})^2 \leq \left(\frac{V_m}{\omega_e}\right)^2. \tag{33}$$

When machine under the load tends to increase its speed, the voltage ellipse "shrinks" reducing the area of reachable current reference vector. In the case when reference current is located outside the voltage ellipse, the increase of current in the direction of negative d axis is required, i.e. field-weakening operation is performed, which in result forces the reference current vector to return inside the voltage ellipse. In order to maintain the desired torque, the q axis component of current should be changed simultaneously with the d

axis current component according to

$$i_q = \frac{T_e}{\frac{3}{2}p(\Psi_{md} + (L_d - L_q)i_d)}. \tag{34}$$

There are infinite current vector values which meet above stated conditions. However, given the nature of PM machine losses, in the field-weakening region minimum loss condition among all current vector combinations is achieved at the intersection of voltage ellipse and torque curve (Figure 6). The solution of field-weakening problem enriched with minimum loss requirement can be found solving the equation obtained by combining (34) and (33).

In the absence of a solution, i.e. non-existence of voltage ellipse and torque curve intersection, the desired torque reference is not reachable and must be adequately altered. In the aforementioned case, solution to the FW problem is the touching point of voltage ellipse and torque curve (Figure 7(a)), formally known as maximum torque per voltage (MTPV) curve.

To ensure that restriction on current amplitude is satisfied, the maximum torque at which machine can operate should be defined. Considering both, the maximum available torque considering voltage and current limit, the operating point of maximum torque per volt and ampere (MTPVA) is defined according to Figure 7(b) at the intersection point of the voltage ellipse and current circle.

With the assumption that flux linkage components in d and q axis are

$$\begin{aligned} \Psi_d &= \hat{\Psi}_d = \Psi_{md} + L_d i_d, \\ \Psi_q &= \hat{\Psi}_q = L_q i_q, \end{aligned} \tag{35}$$

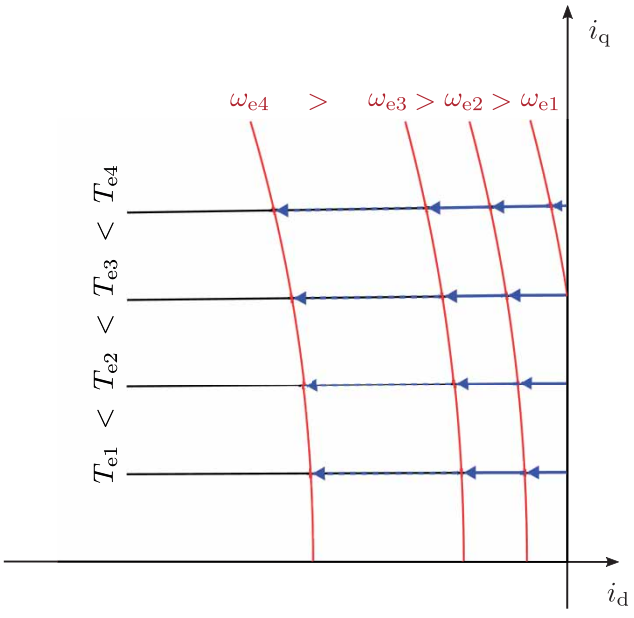

Figure 6. SMPM synchronous machine operation in field-weakening region.

where hat ˆ symbol denotes the presumed values, i.e. inductances and flux linkage which are measured prior to machine exploitation and/or estimated values, it is possible and completely justified to determine the required FW action using equations (33) and (34). Due to inevitable error caused by saturation effects and error in parameter determination, using the described approach results in erroneous FW operation. Additionally, contributing to stated errors and causing faulty FW operation are the neglected voltage drop across winding resistance R_s and the temperature sensitive flux linkage component in the d axis produced by permanent magnets

$$\Psi_{md,T} = \Psi_{md,T_0}(1 - \alpha \Delta T), \tag{36}$$

where $\Psi_{md,T}$ and Ψ_{md,T_0} denote permanent magnet flux linkage at temperatures T and T_0, respectively, ΔT is the magnet temperature rise, while α is the temperature coefficient of remanence (for neodynium magnets $\alpha = 0.12$ %/K). For example, in traction application, the temperature of magnets mounted in a PM machine changes often from environment temperature to the maximum allowable magnet temperature, which can result in temperature difference of $\Delta T = 150$ K and consequently permanent magnet remanence and flux linkage drop of 18%. A novel field-weakening approach which is able to compensate for voltage drop across winding resistance and eventual deviation/error of parameters and flux values from the real ones is presented in the remainder of this section.

4.1. Field weakening algorithm

Combining the PI controller equations (13)–(14) and machine model equations (1)–(2), with addition of steady-state operating condition presumption, i.e. $(i_d^* - i_d) = (i_q^* - i_q) = \frac{\mathrm{d}}{\mathrm{d}t}\Psi_d = \frac{\mathrm{d}}{\mathrm{d}t}\Psi_d = 0$, the current closed-loop model can be expressed as (Figure 8)

$$\begin{aligned} K_{id} I_{ed} &= R_s i_d^* - \omega_e \Delta\Psi_q, \\ K_{id} I_{eq} &= R_s i_q^* + \omega_e \Delta\Psi_d, \end{aligned} \tag{37}$$

where $\Delta\Psi_d$ and $\Delta\Psi_q$ are difference/error between real flux linkages and those calculated using presumed machine parameters

$$\begin{aligned} \Delta\Psi_d &= \Psi_d - \hat{\Psi}_d = \Psi_d - (\Psi_{md} + L_d i_d^*) \\ \Delta\Psi_q &= \Psi_q - \hat{\Psi}_q = \Psi_q - L_q i_q^*. \end{aligned} \tag{38}$$

During field-weakening operation, due to the fact that mechanical time constant is considerably larger than electrical one, the changes in current reference required for field-weakening δi_d and δi_d are small enough so that flux errors $\Delta\Psi_d$ and $\Delta\Psi_q$ between two consecutive time steps along with voltage drop across R_s can be

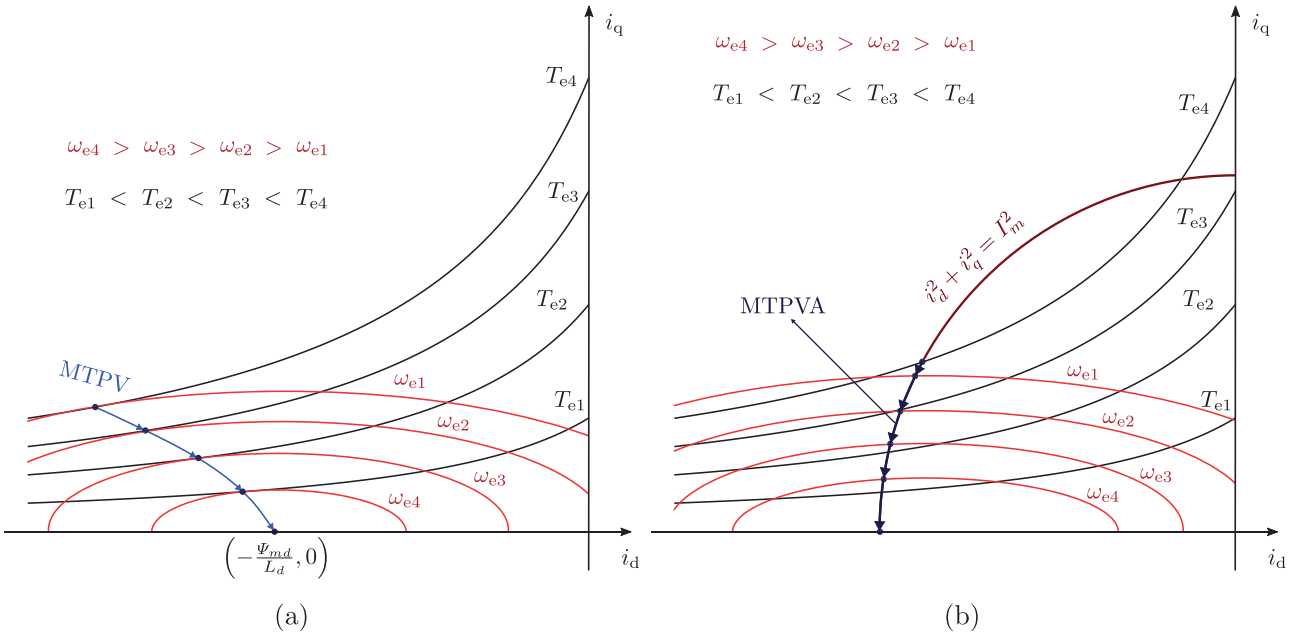

Figure 7. IPM synchronous machine operation in the field-weakening region. (a) MTPV and (b) MTPVA.

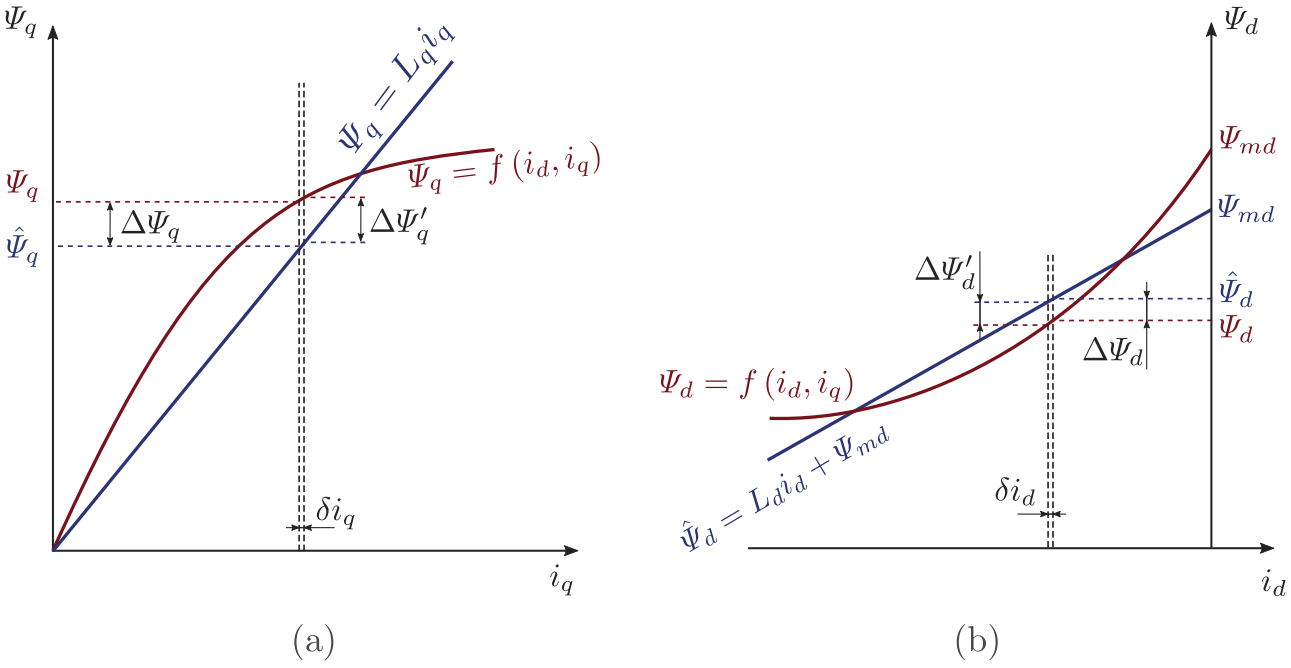

Figure 8. Flux as a function of current: (a) *q* axis and (b) *d* axis flux component.

considered as constant values

$$\begin{aligned} i_d^*(k+1) &= i_d^*(k) + \delta i_d, \\ i_q^*(k+1) &= i_q^*(k) + \delta i_q, \end{aligned} \tag{39}$$

$$\begin{aligned} \Delta\Psi_q(k+1) &= \Delta\Psi_q(k), \\ \Delta\Psi_d(k+1) &= \Delta\Psi_d(k), \end{aligned} \tag{40}$$

$$\begin{aligned} R_s i_d^*(k+1) &= R_s i_d^*(k), \\ R_s i_q^*(k+1) &= R_s i_q^*(k). \end{aligned} \tag{41}$$

Combining (13), (14), (37) and (38), voltage limits can now be reformulated as

$$\begin{aligned} v_d^* &= K_{id} I_{ed}(k) - \omega_e L_q i_q^*, \\ v_q^* &= K_{iq} I_{eq}(k) + \omega_e (\Psi_{md} + L_d i_d^*). \end{aligned} \tag{42}$$

The solution to field-weakening problem can be finally found by solving the optimization problem stated as

$$\begin{aligned} &\min \Gamma(x_r) = h_1 (T_e^* - T_e(x_r))^2 + h_2 (i_d^* - i_{d_{LM}})^2, \\ &\text{s. t. } x_r \in \mathcal{X}_r \end{aligned} \tag{43}$$

with $x_r = [i_d^* \, i_q^*]^\intercal$, $T_e(x_r) = 1.5p(\Psi_{md} + (L_d - L_q)i_d^*)i_q^*$ and $\mathcal{X}^*$ being the set of constraints defined as

$$\mathcal{X}_r = \begin{cases} (v_d^*)^2 + (v_q^*)^2 \leq V_m^2, \\ (i_d^*)^2 + (i_q^*)^2 \leq I_m^2. \end{cases} \tag{44}$$

Variables h_1 and h_2 represents weighting coefficients, T_e^* is the desired torque (torque command) and $i_{d_{LM}}$ is the current reference in d axis at which losses are minimal for the given torque command. In PMSM control algorithm, the loss minimizing d axis current $i_{d_{LM}}$ is usually obtained from a previous measurements or calculations saved in a form of a look-up table. The stated constrained minimization problem is, in the context of this paper, solved using the projected gradient method [27], an iterative search algorithm with iteration defined as

$$\begin{aligned} x_r^{k+1} &= x_r^k + \gamma_k(z_r^k - x_r^k), \\ z_r^k &= P_{\mathcal{X}_r}(x_r^k - \beta_k \nabla \Gamma(x_r^k)), \end{aligned} \tag{45}$$

where β_k and γ_k are the positive stepsizes. Operator $P_{\mathcal{X}_r}$ defines the orthogonal projection onto convex set $\mathcal{X}_r$. For a specified problem, stepsizes β_k and γ_k are, for every iteration k, defined using Armijo search along the boundary $\mathcal{X}_r$, i.e. as

$$\gamma^k = 1, \quad \beta^k = \bar{\beta} 2^{-l(k)}, \tag{46}$$

with

$$\begin{aligned} l(k) = \min\{j \in \mathcal{Z}_{\geq 0} : f(z_r^{k,j}) \leq f(x_r^k) \\ - \sigma \nabla f(x_r^k)^\intercal (x_r^k - z_r^{k,j})\}, \end{aligned} \tag{47}$$

$$z_r^{k,j} = P_{\mathcal{X}_r}(x_r^k - \bar{\beta} 2^{-j} \nabla f(x_r^k)), \tag{48}$$

for some $\bar{\beta} > 0$ and $\sigma \in (0, 1)$.

Table 1. Parameters of the PMSM.

Symbol	Description	Value	Unit
P_n	Nominal power	4.2	kW
n_n	Nominal speed	620	rpm
I_n	Nominal current	28	A
R_s	Stator phase resistance	137	mΩ
L_d	d axis inductance	2.3	mH
L_q	q axis inductance	2.1	mH
λ_m	Permanent magnet flux linkage	410	mVs
p	Pole pairs	4	
f_s	Sampling/switching frequency	12	kHz

5. Results

The verification of the presented field-weakening algorithm and current reference governor was performed in two steps, namely through simulation and through experiment on the real PMSM drive. The simulation was performed using machine model whose parameters match the ones obtained through identification and measurements of the real machine (Table 1). For the experiment (Figure 9), the FW and current control algorithm, along with PI current controllers, SVPWM and all other required background tasks, were implemented on Texas Instruments F28343 200 MHz microcontroller. The current reference governor code is executed within each PWM interrupt routine, i.e. with frequency equal to sampling/switching frequency, while the FW code is executed with frequency $f_{\text{FW}} = f_s/N_{\text{FW}}$. To ensure current dynamics during transient does not affect the FW operation and at the same time machine speed can be considered as a constant value

Figure 9. Experimental setup.

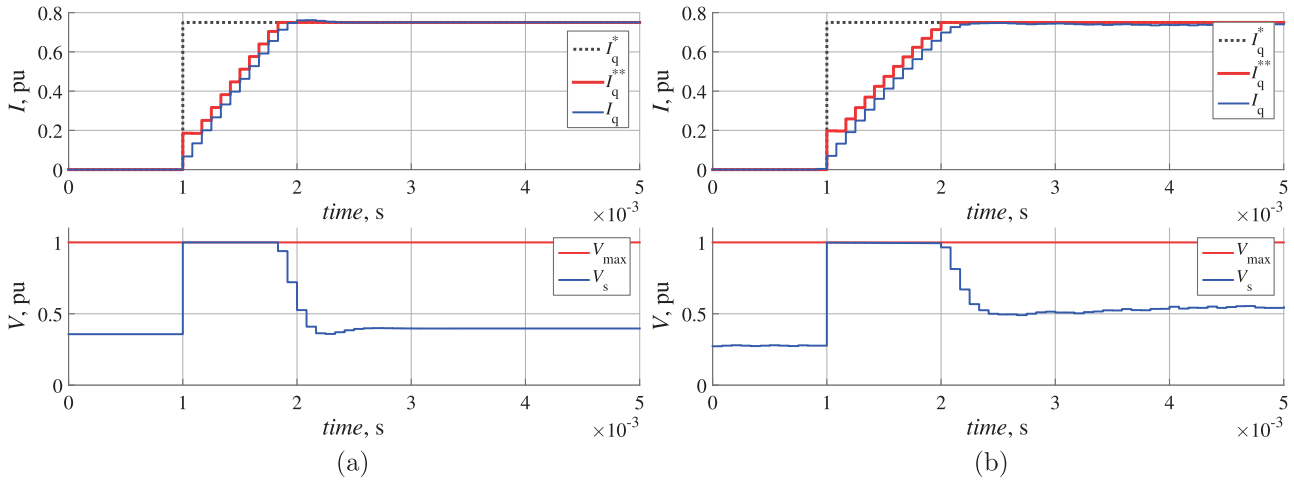

Figure 10. Reference governor results. (a) Simulation and (b) experiment.

between two consecutive FW calculations, the N_{FW} was set to $N_{\mathrm{FW}} = 50$.

The reference governor adaptation (denoted as iq^{**}) of the q axis current reference step change (denoted as iq^{*}), along with the current control actions and the current response iq are evaluated and presented in the upper section of Figure 10. The lower section shows the amplitude of the resulting voltage vector ($\sqrt{v_d^{*2} + v_d^{*2}}$) and its constraint $V_{\max}$ defined by available voltage from the inverter. The d axis current during the experiment is set to zero ($i_d^* = 0$), while the current reference in the q axis i_q^* is proportional to the required torque T_e^*. A comparison of the proposed current control with reference governor and the classic *PI* controller with back-calculation anti-windup can be found in previously published conference paper [18], in which robustness of the current reference governor performance with respect to the motor parameter variation is also presented.

The performance of field-weakening algorithm is presented in Figure 12. During field-weakening experiment, the reference torque, which in case of SMPM is proportional to the current component in the q axis, is kept at a constant value, while the machine speed change is forced with mechanically coupled induction machine (IM) in order to force the FW operation reflected as a change in the d axis current component.

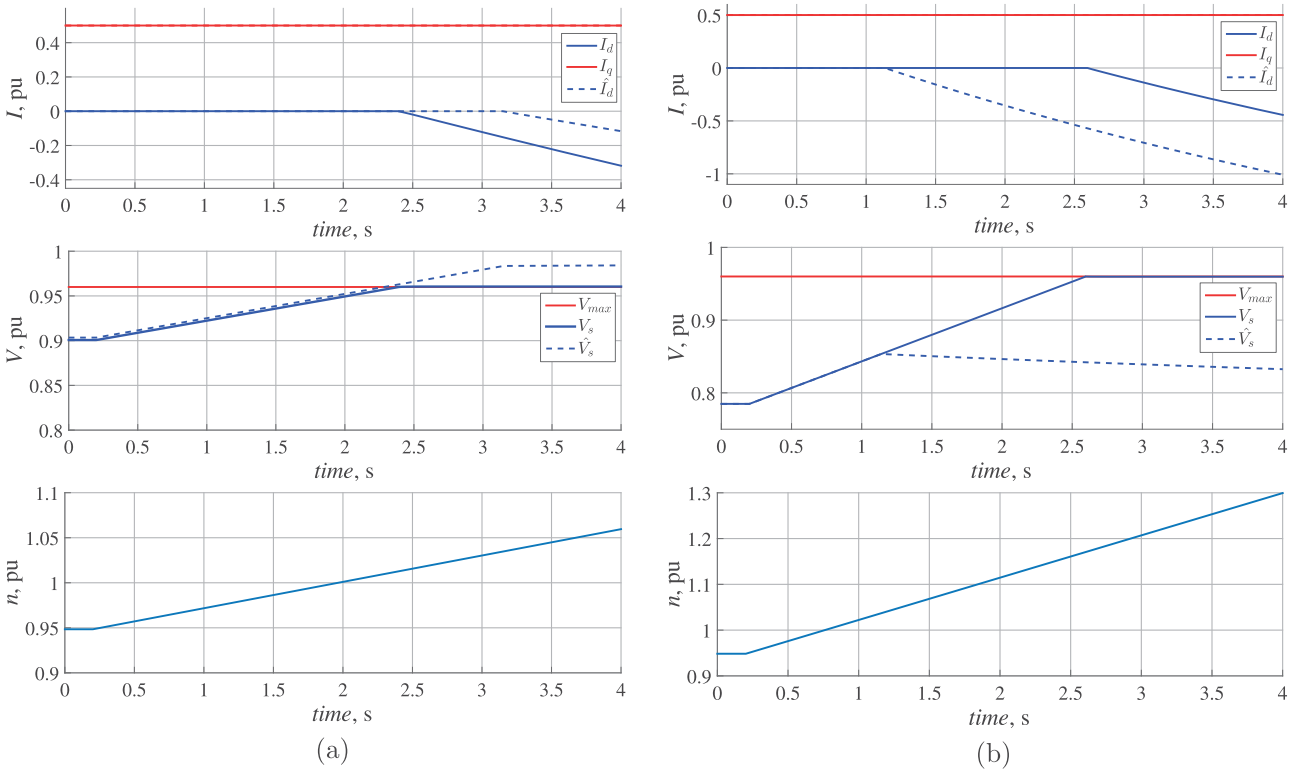

Figure 11. Field-weakening operation with (solid line) and without parameter uncertainty compensation (dashed line) for perturbed motor parameters. (a) Simulation a and (b) Simulation b.

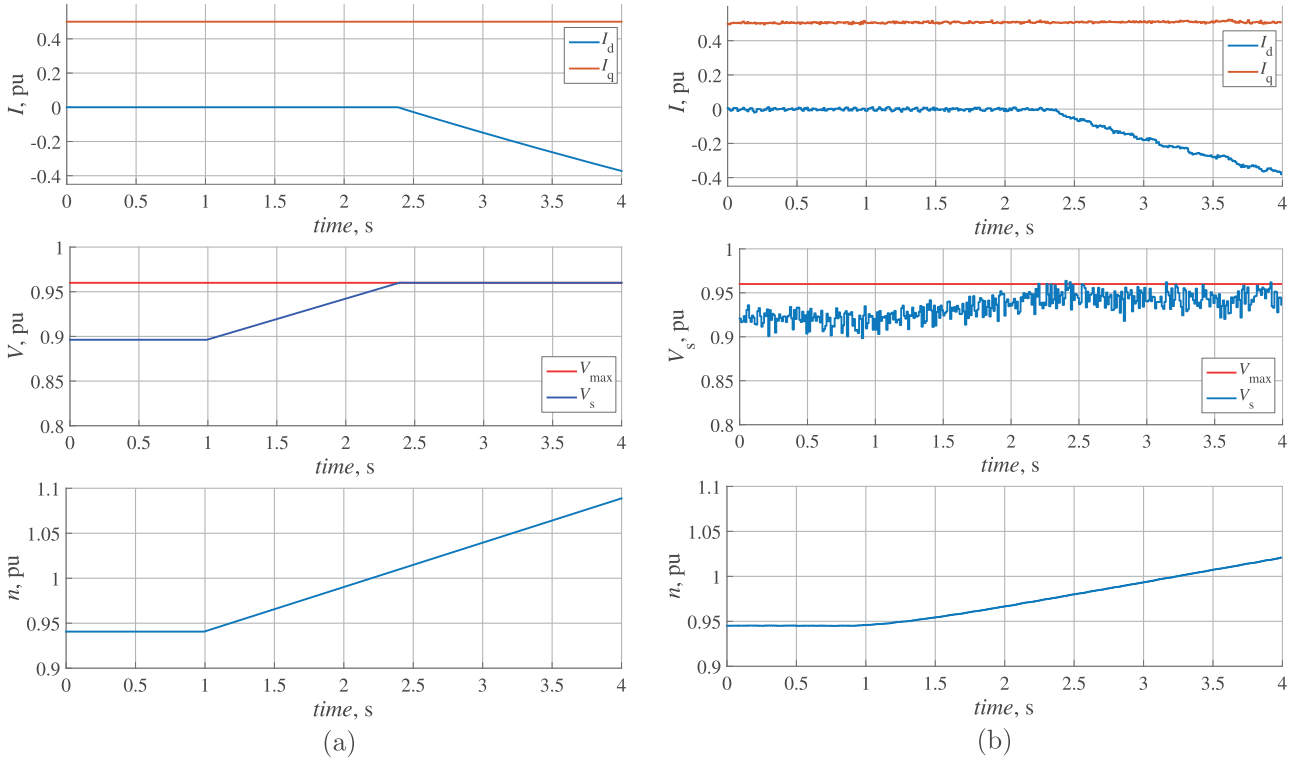

Figure 12. Field weakening operation. (a) Simulation and (b) experiment.

The presented results show the adaptation of the reference current performed by the reference governor which does not result in a violation of the voltage constraint. When comparing Figures 10(b) and 12(b) a different level of noise can be observed. This difference comes from different time scales of the corresponding experiments.

The effectiveness of the proposed parameter uncertainty compensation during field-weakening is investigated in simulation by varying the motor parameters according to Table 2 and compared to field-weakening algorithm without parameter uncertainty compensation. The results are presented in Figure 11. The results point out that the proposed field weakening algorithm is robust to parameter variation while the algorithm without parameter uncertainty compensation is sensitive to variation of the motor parameters. A similar analysis is performed for the reference governor in previously published conference paper [18], where the reference governor is also shown to be robust to variation of the motor parameters.

Due to safety reasons, in order to leave enough voltage reserve for a possible large torque change, i.e. current step change during FW operation, the field-weakening voltage limit is selected as a value lower than the actual limit, which is a common practice in control of permanent magnet synchronous machines.

Table 2. Variated parameters of the PMSM.

	L_d^*	L_q^*	Ψ_{md}^*	R_s^*
Figure 11(a)	$0.7L_d$	$0.7L_q$	Ψ_{md}	R_s
Figure 11(b)	L_d	L_q	$0.7\Psi_{md}$	$1.5R_s$

6. Conclusion

High performance control of PMSMs can be achieved using rotor-field-oriented vector control. Usually, *d* and *q* axis currents are controlled independently using PI controllers with additional decoupling terms. Due to a limited voltage available from the inverter, the current controllers are prone to saturation which leads to disturbed current dynamics, degraded torque production and potentially the system instability. In order to overcome the problem of saturation, the adaptation of current references in the form of a reference governor is implemented in the control structure of a permanent magnet synchronous machine. In order to ensure that voltage and current constraints are not violated in steady state, i.e. to ensure reachability of the torque reference, a novel field-weakening algorithm is introduced. The presented algorithms are robust to parameter changes, thereby allowing the use of incorrectly assessed motor parameters and implementation on the motor with a high degree of saturation. The field-weakening and current reference governor algorithm are implemented on Texas Instruments F28343 200 MHz microcontroller and experimentally verified on surface mounted permanent magnet motor drive.

Disclosure statement

No potential conflict of interest was reported by the authors.

Funding

This work was supported in part by the Croatian Science Foundation under the Project IP-11-2013-7801 Advanced Electric Drives for Traction Applications.

References

[1] Lee J, Nam K, Choi S, et al. A lookup table based loss minimizing control for FCEV permanent magnet synchronous motors. Vehicle Power and Propulsion Conference, 2007; VPPC 2007; IEEE; 2007. p. 175–179.

[2] Jung SY, Hong J, Nam K. Current minimizing torque control of the IPMSM using Ferrari's method. IEEE Trans Power Electron. 2013;28(12):5603–5617.

[3] Cao M. Online loss minimization control of IPMSM for electric scooters. Power Electronics Conference (IPEC), 2010 International. IEEE; 2010. p. 1388–1392.

[4] Uddin MN, Zou H, Azevedo F. Online loss-minimization-based adaptive flux observer for direct torque and flux control of PMSM drive. IEEE Trans Ind Appl. 2016;52(1):425–431.

[5] French C, Acarnley P. Direct torque control of permanent magnet drives. IEEE Trans Ind Appl. 1996;32(5): 1080–1088.

[6] Merzoug M, Naceri F. Comparison of field-oriented control and direct torque control for permanent magnet synchronous motor (PMSM). Proceedings of World Academy of Science, Engineering and Technology; Vol. 35. Citeseer; 2008. p. 299–304.

[7] Harnefors L, Nee HP. Model-based current control of AC machines using the internal model control method. IEEE Trans Ind Appl. 1998;34(1):133–141.

[8] Seok JK, Kim JS, Sul SK. Overmodulation strategy for high-performance torque control. IEEE Trans Power Electron. 1998;13(4):786–792.

[9] Briz F, Diez A, Degner M, et al. Current and flux regulation in field-weakening operation [of induction motors]. IEEE Trans Ind Appl. 2001;37(1):42–50.

[10] Preindl M, Bolognani S. Comparison of direct and PWM model predictive control for power electronic and drive systems. Applied Power Electronics Conference and Exposition (APEC), 2013 Twenty-Eighth Annual IEEE; 2013. p. 2526–2533.

[11] Yan Y, Wang S, Xia C, et al. Hybrid control set-model predictive control for field-oriented control of VSI-PMSM. IEEE Trans Energy Convers. 2016;31(4): 1622–1633.

[12] Slapak V, Kyslan K, Durovsky F. Position controller for PMSM based on finite control set model predictive control. Elektronika ir Elektrotechnika. 2016;22(6): 17–21.

[13] Mariéthoz S, Domahidi A, Morari M. Sensorless explicit model predictive control of permanent magnet synchronous motors. Electric Machines and Drives Conference, 2009; IEMDC'09; IEEE International. IEEE; 2009. p. 1250–1257.

[14] Richter S, Mariéthoz S, Morari M. High-speed online MPC based on a fast gradient method applied to power converter control. American Control Conference (ACC), 2010. IEEE; 2010. p. 4737–4743.

[15] Preindl M, Bolognani S, Danielson C. Model predictive torque control with PWM using fast gradient method. Applied Power Electronics Conference and Exposition (APEC), 2013 Twenty-Eighth Annual IEEE. IEEE; 2013. p. 2590–2597.

[16] Kolmanovsky I, Garone E, Di Cairano S. Reference and command governors: a tutorial on their theory and automotive applications. American Control Conference (ACC), 2014. IEEE; 2014. p. 226–241.

[17] Gilbert EG, Tan KT. Linear systems with state and control constraints: the theory and application of maximal output admissible sets. IEEE Trans Automat Control. 1991;36(9):1008–1020.

[18] Jerčić T, Ileš Š, Žarko D, et al. Current reference governor of permanent magnet synchronous machine. 2016 XXII International Conference on Electrical Machines (ICEM). IEEE; 2016. p. 1022–1028.

[19] Pan CT, Sue SM. A linear maximum torque per ampere control for IPMSM drives over full-speed range. IEEE Trans Energy Convers. 2005;20(2):359–366.

[20] Bech MM, Frederiksen TS, Sandholdt P. Accurate torque control of saturated interior permanent magnet synchronous motors in the field-weakening region. Industry Applications Conference, 2005. Fourtieth IAS Annual Meeting. Conference Record of the 2005; Vol. 4. IEEE; 2005. p. 2526–2532.

[21] Macminn SR, Jahns TM. Control techniques for improved high-speed performance of interior PM synchronous motor drives. Industry Applications Society Annual Meeting, 1988; Conference Record of the 1988 IEEE. IEEE; 1988. p. 272–280.

[22] Simanek J, Novak J, Cerny O, et al. FOC and flux weakening for traction drive with permanent magnet synchronous motor. IEEE International Symposium on Industrial Electronics, 2008. ISIE 2008. IEEE; 2008. p. 753–758.

[23] Jevremovic V, Marcetic D. Closed-loop flux-weakening for permanent magnet synchronous motors. 4th IET International Conference on Power Electronics, Machines and Drives (PEMD 2008). IET; 2008. p. 717–721.

[24] Lenke RU, De Doncker RW, Mu-Shin K, et al. Field weakening control of interior permanent magnet machine using improved current interpolation technique. Proc. IEEE PESC; 2006. p. 1–5.

[25] Yamakawa T, Wakao S, Kondo K, et al. A new flux weakening operation of interior permanent magnet synchronous motors for railway vehicle traction. 2005 European Conference on Power Electronics and Applications. IEEE; 2005. p. 6–pp.

[26] Bae BH, Patel N, Schulz S, et al. New field weakening technique for high saliency interior permanent magnet motor. Industry Applications Conference, 2003. Conference Record of the 38th IAS Annual Meeting; Vol. 2. IEEE; 2003. p. 898–905.

[27] Iusem A. On the convergence properties of the projected gradient method for convex optimization. Comput Appl Math. 2003;22(1):37–52.